Short-term synaptic depression and stochastic vesicle dynamics reduce and shape neuronal correlations

Robert Rosenbaum, Jonathan E. Rubin and Brent Doiron

J Neurophysiol 109:475-484, 2013. First published 31 October 2012;
doi: 10.1152/jn.00733.2012

Journal of Neurophysiology publishes original articles on the function of the nervous system. It is published 24 times a year (twice monthly) by the American Physiological Society, 9650 Rockville Pike, Bethesda MD 20814-3991. ESSN: 1522-1598. Visit our website at http://www.the-aps.org/.

J Neurophysiol 109: 475–484, 2013.
First published October 31, 2012; doi:10.1152/jn.00733.2012.

Short-term synaptic depression and stochastic vesicle dynamics reduce and shape neuronal correlations

Robert Rosenbaum, Jonathan E. Rubin, and Brent Doiron
Department of Mathematics, University of Pittsburgh, Pittsburgh, Pennsylvania

Submitted 21 August 2012; accepted in final form 29 October 2012

Rosenbaum R, Rubin JE, Doiron B. Short-term synaptic depression and stochastic vesicle dynamics reduce and shape neuronal correlations. *J Neurophysiol* 109: 475–484, 2013. First published October 31, 2012; doi:10.1152/jn.00733.2012.—Correlated neuronal activity is an important feature in many neural codes, a neural correlate of a variety of cognitive states, as well as a signature of several disease states in the nervous system. The cellular and circuit mechanics of neural correlations is a vibrant area of research. Synapses throughout the cortex exhibit a form of short-term depression where increased presynaptic firing rates deplete neurotransmitter vesicles, which transiently reduces synaptic efficacy. The release and recovery of these vesicles are inherently stochastic, and this stochasticity introduces variability into the conductance elicited by depressing synapses. The impact of spiking and subthreshold membrane dynamics on the transfer of neuronal correlations has been studied intensively, but an investigation of the impact of short-term synaptic depression and stochastic vesicle dynamics on correlation transfer is lacking. We find that short-term synaptic depression and stochastic vesicle dynamics can substantially reduce correlations, shape the timescale over which these correlations occur, and alter the dependence of spiking correlations on firing rate. Our results show that short-term depression and stochastic vesicle dynamics need to be taken into account when modeling correlations in neuronal populations.

correlation transfer; short-term synaptic depression; spike-train correlation; synaptic filtering

CORRELATIONS BETWEEN THE SPIKING activity of cortical neurons is a signature feature of sensory coding (Averbeck et al. 2006), attentional modulation (Cohen and Maunsell 2009; Mitchell et al. 2009), as well as working memory and decision making (Romo et al. 2003; Polk et al. 2012; Cain and Shea-Brown 2012). Correlations between the spiking activity of cortical neurons have important consequences for sensory coding and attention. Subthreshold membrane potential fluctuations and spike trains of nearby neurons exhibit significant correlated variability (Mastronarde 1983; Zohary et al. 1994; Lampl et al. 1999; Bair et al. 2001; Kohn and Smith 2005; Shlens et al. 2006; Okun and Lampl 2008; Poulet and Petersen 2008; Cohen and Maunsell 2009; Ranganathan and Koester 2011). Nevertheless, there is a recent debate over the degree to which cortical spike trains are correlated in awake, behaving animals (Ecker et al. 2010; Renart et al. 2010; Cohen and Kohn 2011). Due to the difficulty of obtaining accurate estimates of spiking correlations in vivo (Ecker et al. 2010; Cohen and Kohn 2011) and the obscurity of the sources of correlations measured in complicated networks, computational modeling plays an important role in understanding how correlations arise in networks and how they are affected by various neural mechanisms. Computational studies have been successful at identifying a number of mechanisms that impact the amplitude and structure of correlations in neuronal networks (Binder and Powers 2001; Moreno-Bote and Parga 2006, 2009; de la Rocha et al. 2007; Renart et al. 2010; Rosenbaum et al. 2010; Tchumatchenko et al. 2010; Litwin-Kumar et al. 2011; Rosenbaum and Josíc 2011; Macke et al. 2011; Pernice et al. 2011; Ly et al. 2012; Tetzlaff et al. 2012; Trousdale et al. 2012), but the impact of short-term synaptic depression on neuronal correlations has not been systematically addressed in the literature.

Synaptic neurotransmitter vesicles are released probabilistically in response to a presynaptic spike, and released vesicles are recovered stochastically over a timescale of several hundred milliseconds (Vere-Jones 1966; Wang 1999; Fuhrmann et al. 2002; Goldman 2004; Rosenbaum et al. 2012). The depletion of neurotransmitter vesicles by trains of presynaptic action potentials gives rise to a form of short-term synaptic depression that is pervasive in the cortex (Zucker and Regehr 2002). We find that when two postsynaptic neurons receive correlated input through depressing synapses, the correlation between the synaptic conductances across the neurons' membranes, as well as the neurons' spike trains, are drastically smaller than the correlations predicted by a nondepressing, static synapse model. This reduction in correlation is especially prevalent at higher presynaptic firing rates that more effectively deplete neurotransmitter vesicles. Coupled with the fact that cellular dynamics suppress correlations at low firing rates (de la Rocha et al. 2007), these results show that a population of neurons with depressing synapses exhibit small correlations over a broad range of firing rates, even when their inputs are strongly correlated. Our conclusions reveal an important, yet often ignored, mechanism that promotes asynchronous spiking activity in densely connected neuronal populations.

METHODS

We begin by describing the statistical measures used to quantify correlations in this study. We then describe the presynaptic population model, synapse model, and neuron model used in this study. Throughout, we use analytical results from (Rosenbaum et al. 2012) to find a closed form approximation to the statistics of the synaptic conductances generated by the presynaptic population.

Statistical measures of temporal correlations. Temporal correlations are measured using the cross-covariance function, defined by

$$C_{xy}(\tau) = \mathrm{cov}[x(t), y(t+\tau)]$$

for any two stationary processes, $x(t)$ and $y(t)$. The cross-covariance between a process and itself is called and autocovariance and denoted $A_x(\tau) := C_{xx}(\tau)$. When $x(t) = \sum_i \delta(t - t_i)$ is a point process represent-

Address for reprint requests and other correspondence: R. Rosenbaum, Dept. of Mathematics, Univ. of Pittsburgh, 301 Thackeray Hall, Pittsburgh, PA 15260 (e-mail: robertr@pitt.edu).

ing a spike train, the spike counting process is defined by $N_x(t) = \int_O^t x(s)ds$ and represents the number of spikes emitted during a time window of duration t. If both $x(t)$ and $y(t)$ are spike trains, then the spike count covariance is defined by (Tetzlaff et al. 2008)

$$\gamma_{xy}(t) = \mathrm{cov}\left[N_x(t), N_y(t)\right] = \int_{-t}^{t} C_{xy}(\tau)(t - |\tau|)d\tau \qquad (1)$$

and the spike count variance is denoted $\sigma_x^2(t) := \gamma_{xx}(t)$. The spike count correlation is then defined as

$$\rho_{xy}(t) = \frac{\gamma_{xy}(t)}{\sigma_x(t)\sigma_y(t)} \qquad (2)$$

and represents the Pearson correlation coefficient between the number of spikes in a time window of duration t. Even though the definitions of $\sigma_x(t)$, $\gamma_{xy}(t)$, and $\rho_{xy}(t)$ were motivated by the interpretation of $N_x(t)$ and $N_y(t)$ as spike counts, we extend their usage to cases in which $x(t)$ and $y(t)$ represent synaptic conductances instead of spike trains. We refer to this measure as the Pearson correlation over a window of size t.

Static synapse model. To study the effects of synaptic depression on correlations, we compare results for a depressing model described below to results for a nondepressing, static synapse model described here. The synaptic conductance produced by a presynaptic spike train, $x(t) = \sum_j \delta(t - t_j)$, for this static model is given by

$$g(t) = \sum_j w\alpha(t - t_j)$$

where w is a constant.

When $x(t)$ is a Poisson process with rate ν, the autocovariance function of the conductance is given by (Tetzlaff et al. 2008)

$$A_g(\tau) = \nu w^2(\alpha \bigstar \alpha)(\tau)$$

where $\bigstar$ denotes cross-correlation, $(f \bigstar g)(\tau) = \int f(t)g(t + \tau)dt$. The cross-covariance function between two conductances driven by a pair of spike trains, $x(t)$ and $y(t)$, is given by

$$C_{gg}(\tau) = w^2[C_{in} * (\alpha_x \bigstar \alpha_y)](\tau)$$

where $C_{\mathrm{in}}(\tau)$ is the cross-covariance between the presynaptic inputs, $x(t)$ and $y(t)$, and * denotes convolution, $(f * g)(\tau) = \int f(t)g(\tau - t)dt$.

Depressing synapse model. A widely used model of short-term synaptic depression captures only the trial-averaged synaptic response to a presynaptic spike train (Tsodyks and Markram 1997). Since we are concerned with neural variability in this work, we use a more detailed model that captures the trial-to-trial variability introduced by probabilistic vesicle release and stochastic recovery times (Vere-Jones 1966; Wang 1999; Fuhrmann et al. 2002; Goldman 2004; de la Rocha and Parga 2005; Rosenbaum et al. 2012).

A presynaptic neuron makes M functional contacts onto a postsynaptic neuron. Each functional contact can dock at most one neurotransmitter vesicle at a time. When a presynaptic spike arrives, each docked vesicle is released with probability p_r. After releasing a docked vesicle, a contact enters a refractory period in which it is unable to release another vesicle. Recovery from this refractory period occurs as a Poisson process with rate $1/\tau_u$. In other words, the duration of the refractory period at a single synaptic contact is exponentially distributed with mean τ_u. Let $x(t) = \sum_j \delta(t - t_j)$ be the presynaptic spike train that drives the synapse and define $w_j \in [0, M]$ to be the number of vesicles released by the jth presynaptic spike. Then the synaptic conductance generated by $x(t)$ is given by

$$g(t) = \sum_j w_j\alpha(t - t_j),$$

where t_j is the jth presynaptic spike time and $\alpha(t)$ is a postsynaptic conductance kernel that represents the conductance generated by the release of a single excitatory neurotransmitter vesicle.

Assuming that the presynaptic spike train is a Poisson process with rate ν, an approximation to the autocovariance function of the synaptic conductance is given by (Rosenbaum et al. 2012; Merkel and Lindner 2010)

$$A_g(\tau) = \mathrm{cov}[g(t), g(t + \tau)] = \left\{\left[\nu(1 + D_0)(K \bigstar K) + F\right] * (\alpha \bigstar \alpha)\right\}(\tau).$$

The kernel $K(\tau)$ represents the temporal filtering effects of short-term depression and takes the form of a delta function added to a negative exponential (Rosenbaum et al. 2012),

$$K(\tau) = A_K\delta(\tau) - B_K e^{-\tau/\tau_0}\Theta(\tau),$$

where $\Theta(\tau)$ is the Heaviside step function. The additive term, $F(\tau)$, represents the effects of stochastic vesicle recovery and probabilistic release on the temporal variability of the synaptic response and takes the form (Rosenbaum et al. 2012)

$$F(\tau) = A_F\delta(\tau) - B_F e^{-|\tau|/\tau_0}.$$

Expressions for the constants D_0, τ_0, A_K, B_K, A_F, and B_F are given in the APPENDIX.

Since we are interested in correlations between neuronal responses, we also must consider the cross-covariance between two conductances produced by two correlated presynaptic spike trains, $x(t)$ and $y(t)$ (Fig. 1). For the purposes of this study, we can assume that the two spike trains are Poisson with the same rate, ν. An approximation to the cross-covariance between the two synaptic conductances they produce is given by (Rosenbaum et al. 2012)

$$C_{gg}(\tau) = (1 + c_0D_0)[(K \bigstar K) * (\alpha \bigstar \alpha) * C_{\mathrm{in}}](\tau).$$

where $C_{\mathrm{in}}(\tau)$ is the cross-covariance function between the input spike trains, $x(t)$ and $y(t)$. The kernel, $K(\tau)$, is defined above and the constants, D_0 and c_0, are given in the APPENDIX. The Pearson correlation, $\rho_{gg}(t)$, between conductances is an analog to spike count correlations between spike trains and can be calculated from the auto- and cross-covariance functions above using *Eqs. 1* and *2*.

Presynaptic population model. We consider a simple presynaptic population model in which two postsynaptic neurons each receive input from n_e excitatory and n_i inhibitory presynaptic neurons (Fig. 2*A*). Synaptic conductances are denoted using the letter g. Generally, presynaptic spike counts and postsynaptic conductances from individual presynaptic neurons are denoted with lowercase letters and subscripts (e for excitatory and i for inhibitory), whereas population-level spike counts and postsynaptic conductances, obtained by summing individual spike counts and conductances, are denoted with capital letters and subscripts (E for excitatory and I for inhibitory). The subscript, out, is used for quantities related to the spiking response of postsynaptic neurons. The subscript, in, is used for quantities, like firing rates, that are identical for excitatory and inhibitory presynaptic inputs.

We denote the jth presynaptic excitatory input spike train to postsynaptic neuron k by $e_{k,j}(t)$ for $j = 1, 2, \ldots, n_e$ and $k = 1, 2$. The inhibitory inputs are denoted analogously. For simplicity, we assume that all of the presynaptic spike trains are Poisson processes. Excitatory and inhibitory spike trains have rate ν_{in} and the autocovariance of these Poisson inputs is given by $A_{\mathrm{in}}(\tau) = \nu_{\mathrm{in}}\delta(\tau)$.

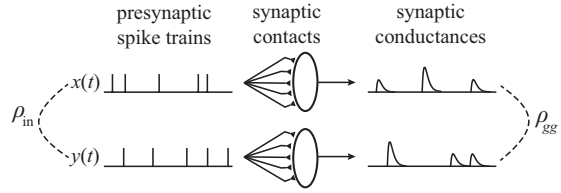

Fig. 1. Model for synaptic correlation transfer with two presynaptic spike trains. Two correlated presynaptic spike trains, $x(t)$ and $y(t)$, each drive $M = 5$ synaptic contacts to produce two synaptic conductance traces. We are interested in how the correlation, $\rho_{\mathrm{in}}(t)$, between the presynaptic spike trains is transferred to the correlation, $\rho_{gg}(t)$, between the synaptic conductances.

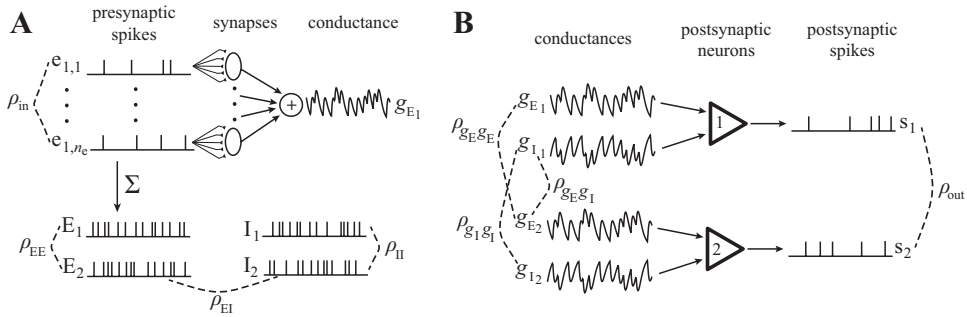

Fig. 2. Presynaptic population model. *A*: each of $n_e = 150$ presynaptic spike trains drives $M = 5$ synaptic contacts to produce the first neuron's total excitatory synaptic conductance, $g_{E,1}(t)$. The sum of these presynaptic spike trains is denoted $E_1(t)$ and similarly for $E_2(t)$, $I_1(t)$, and $I_2(t)$. Every pair of presynaptic spike trains is correlated with coefficient, $\rho_{in}(t)$. Correlation between the excitatory population spike trains is denoted $\rho_{EE}(t)$ and similarly for $\rho_{II}(t)$ and $\rho_{EI}(t)$. *B*: population conductances, $g_{E,2}(t)$, $g_{I,1}(t)$, and $g_{I,2}(t)$ are constructed analogously to $g_{E,1}(t)$ in *A* and their pairwise correlations are denoted $\rho_{g_E g_E}(t)$, $\rho_{g_I g_I}(t)$, and $\rho_{g_E g_I}(t)$. Population conductances drive two postsynaptic neurons to produce two output spike trains, $s_1(t)$ and $s_2(t)$, with correlation given by $\rho_{out}(t)$. We are interested in how $\rho_{in}(t)$ is transferred to $\rho_{out}(t)$.

Each pair of presynaptic spike trains is correlated with cross-covariance function $C_{in}(\tau) = c\nu_{in}e^{-|\tau|/\tau_{corr}}/(2\tau_{corr})$ where c is the total input correlation. Correlated presynaptic spike times are obtained for simulations using a jittered "multiple interaction" scheme (Kuhn et al. 2003). First, a mother Poisson process with rate ν_{in}/c is generated, then each spike train is generated by choosing a proportion c of the spike times from the mother train. After this, every spike time from each population is "jittered" by adding independent exponentially distributed random numbers with mean τ_{corr} (Bäuerle and Grübel 2005).

The normalized covariance, $\gamma_{in}(t)$, between two presynaptic spike counts can be computed from $C_{in}(\tau)$ using *Eq. 1*. Since each presynaptic spike train is a Poisson process, the spike count variances are given by $\sigma^2_{in}(t) = t\nu_{in}$. As a result, the Pearson correlation coefficient between spike counts from excitatory inputs is given by $\rho_{in}(t) = \gamma_{in}(t)/(t\nu_{in})$.

The total number of excitatory presynaptic spikes received by neuron k during the time interval $[0, t]$ is given by

$$N_{E,k}(t) = \sum_{j=1}^{n_e} N_{e,k,j}(t)$$

and similarly for the total number of inhibitory spikes, $N_{I,k}(t)$. The spike count correlations between the total excitatory and between the total inhibitory inputs are given by (Renart et al. 2010; Rosenbaum et al. 2011),

$$\rho_{XX}(t) = \frac{\mathrm{cov}\left[N_{X,1}(t), N_{X,2}(t)\right]}{\sqrt{\mathrm{var}\left[(N_{X,1}(t))\ \mathrm{var}(N_{X,2}(t))\right]}} = \frac{\rho_{in}(t)}{\rho_{in}(t) + \frac{1}{n_x}\left[1 - \rho_{in}(t)\right]}.$$

for $X = E, I$ and $x =$ e, i respectively. Similarly, the spike count correlation between the total excitatory and inhibitory inputs is given by

$$\rho_{EI}(t) = \left\{\rho_{in}(t) + \frac{1}{n_e}\left[1 - \rho_{in}(t)\right]\right\}^{-1/2} \left\{\rho_{in}(t) + \frac{1}{n_i}\left[1 - \rho_{in}(t)\right]\right\}^{-1/2} \rho_{in}(t).$$

The marginal and joint statistics of the individual conductances are given in the previous two sections. The summed excitatory and inhibitory synaptic conductances across the membrane of postsynaptic neuron k are given by

$$g_{E,k}(t) = \sum_{j=1}^{n_e} g_{e,k,j}(t)$$

and

$$g_{I,k}(t) = \sum_{j=1}^{n_i} g_{i,k,j}(t)$$

respectively for $k = 1, 2$. These conductances are used to drive a pair of model postsynaptic neurons (see below and Fig. 2*B*) The Pearson correlation between the total conductances over a window of size t (see above) is given by

$$\rho_{g_X g_X}(t) = \frac{\rho_{g_x g_x}(t)}{\rho_{g_x g_x}(t) + \frac{1}{n_e}\left[1 - \rho_{g_x g_x}(t)\right]},$$

for $X = E, I$ and $x =$ e, i respectively, and

$$\rho_{g_E g_I}(t) = \left\{\rho_{g_e g_i}(t) + \frac{1}{n_e}\left[1 - \rho_{g_e g_i}(t)\right]\right\}^{-1/2} \left\{\rho_{g_e g_i}(t) + \frac{1}{n_i}\left[1 - \rho_{g_e g_i}(t)\right]\right\}^{-1/2} \rho_{g_e g_i}(t).$$

Neuron model. To generate postsynaptic spike times, we use a conductance-based integrate-and-fire neuron model (Dayan and Abbott 2001). The membrane potentials obey

$$C_m \frac{dV_k}{dt} = -g_L(V_k - V_L) - g_{E,k}(t)(V_k - V_E) - g_{I,k}(t)(V_k - V_I)$$

for $k = 1, 2$ where $g_{E,k}(t)$ and $g_{I,k}(t)$ are the excitatory and inhibitory conductances defined above. Each time the membrane potential reaches threshold at Vth, a spike is recorded, the membrane potential is reset to V_{re} and remains there for a refractory period of duration τ_{ref}. The output spike trains are given by

$$s_k(t) = \sum_j \delta(t - t_{k,j})$$

where $t_{k,j}$ is the time of the jth threshold crossing of neuron $k = 1, 2$. We denote the postsynaptic firing rate as ν_{out} and the spike count correlation between two postsynaptic neurons over a window of size t as $\rho_{out}(t)$.

Due to the nonwhite nature of the synaptic conductances, the statistics of the membrane potentials, spike trains, and synaptic currents are difficult to obtain analytically. In particular, the conductances produced by our model contain a quickly decaying positive peak at the origin surrounded by a negative component that decays more slowly (Fig. 3*H*). To the authors' knowledge, there are no

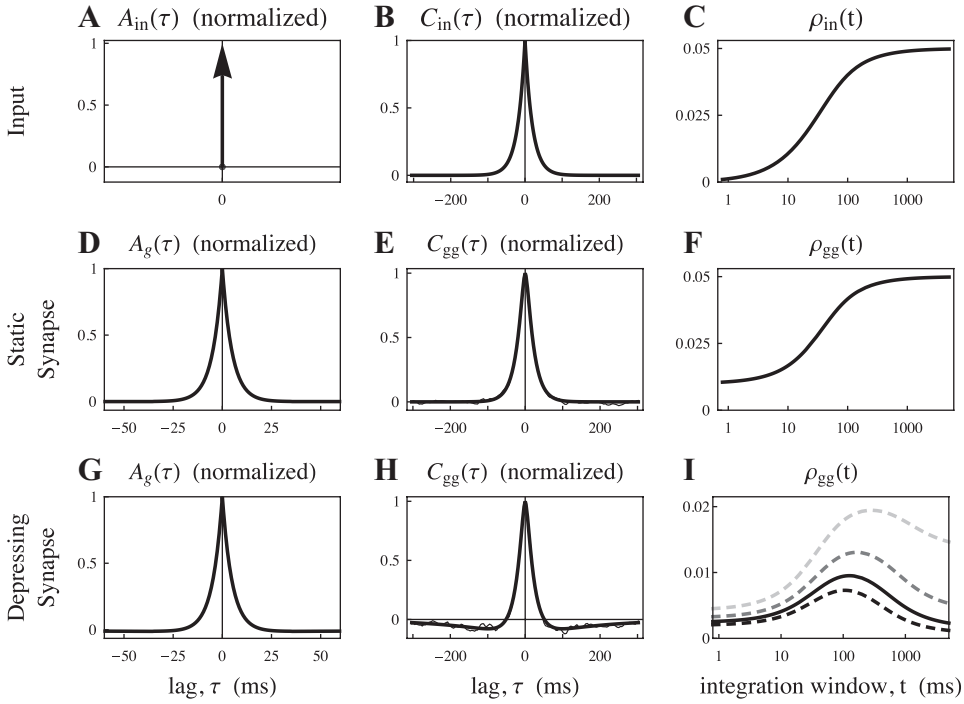

Fig. 3. Short-term depression reduces correlations between a pair of synaptic conductances. Autocovariance (*A*), cross-covariance (*B*), and spike count correlation (*C*) between two Poisson presynaptic spike trains. Vertical arrow in *A* represents a Dirac delta function. *D–F*: autocovariance function, cross-covariance function, and Pearson correlation (see METHODS) for the conductances produced by the presynaptic spike trains in *A–C* using a nondepressing, static synapse model. *G–I*: same, but for a synapse model that exhibits short-term depression with stochastic vesicle dynamics. All solid lines are for a presynaptic rate of ν_{in} = 15 Hz. In *I*, the correlation is shown at three additional presynaptic rates, ν_{in} =5, 10, and 20 Hz (dashed curves; rate increases with darkness of curves). All auto- and cross-covariance functions are normalized to have a maximum at one. Auto- and cross-covariance functions from Monte Carlo simulations are plotted along with those obtained from the analytical expressions in the METHODS, but the two are virtually indistinguishable. Synaptic depression drastically reduces correlations between the conductances, especially over longer time windows.

known analytical methods for obtaining spiking statistics given presynaptic correlations with this temporal structure, so we use Monte Carlo simulations in place of closed form expressions.

An attempt was made to obtain analytical approximations to the spiking statistics using a simpler model and existing theoretical calculations. If we assume instantaneous synapses [$\alpha(t) = JC_m\delta(t)$], Poisson inputs, and delta-correlated input spike trains [$C_{in}(\tau) = c\nu_{in}\delta(\tau)$] our synapse model produces synaptic conductances with correlation functions that consist of a delta function at the origin surrounded by negative exponentially decaying peak. Analytical methods exist to approximate the spiking statistics of current-based integrate-and-fire neurons receiving synaptic currents with correlation functions that have such a shape (Moreno et al. 2002; Moreno-Bote and Parga 2006, 2009). We performed Monte Carlo simulations with a current-based integrate-and-fire neuron where the synaptic current was taken to be proportional to the conductance predicted by our synaptic model with instantaneous synapses and delta correlated inputs. We compared the statistics calculated from these simulations to those obtained using the analytical approximations mentioned above but found substantial disagreement between the simulations and theoretical approximations. These analytical approximations rely on an assumption that the integral of the negative exponential peak in the correlation functions is much smaller than the mass of the delta function. We speculate that the disagreement between our simulations and these approximations to a violation of this assumption in our model but note the possibility that the approximations could be accurate in other parameter regimes where this assumption is not violated. Parameters values used in this study.

Unless otherwise specified, input parameters for all figures are n_e = 150, n_i = 50, c = 0.05, τ_{corr} = 20 ms, and ν_{in} = 15 Hz. The vesicle recovery timescale, τ_u, for nonfacilitating synapses in the cortex is commonly reported to be within the range of 300–1,500 ms and the probability of release at a single contact, p_r, can lie anywhere in the range of 0.1–0.9 (Tsodyks and Markram 1997; Markram 1997; Varela et al. 1997; Fuhrmann et al. 2002; Hanson and Jaeger 2002). Consistent with these findings, we set τ_u = 700 ms and p_r = 0.3. We set the number of functional contacts that each presynaptic cell makes to a postsynaptic cell to M = 5, which is within the ranges observed across many cell types and cortical areas (Branco and Staras 2009). Postsynaptic neuron parameters are V_L = −64 mV, V_{th} = −54 mV, V_{re} = −64 mV, and τ_{ref} = 2 ms. The membrane capacitance and leak conductance are chosen so that $\tau_m = C_m/gL$ = 15 ms. The excitatory postsynaptic conductance kernel is an exponential of the form

$$\alpha_e(t) = \frac{J_e C_m}{\tau_\alpha}\Theta(t)e^{-t/\tau_\alpha}$$

and similarly for the inhibitory postsynaptic conductance kernel,

$$\alpha_i(t) = \frac{J_i C_m}{\tau_\alpha}\Theta(t)e^{-t/\tau_\alpha}$$

where τ_α = 5 ms, J_e = 0.0205, J_i = 0.0504, and $\Theta(t)$ is the Heaviside step function. For the static synapse model we set w = 0.278. These parameter values were chosen so that the postsynaptic firing rate was approximately equal to the presynaptic rate, $\nu_{out} \approx$ 15 Hz, for both the static and depressing synapse models (more precisely, ν_{out} = 15.03 ± 0.0056 Hz for the depressing synapse model and ν_{out} = 15.41 ± 0.0065 Hz for the static synapse model).

To compare postsynaptic spiking correlations produced by the static and depressing models at various postsynaptic firing rates, we varied the presynaptic firing rate from ν_{in} = 0.05 Hz to ν_{in} = 50 Hz. All other parameters were unchanged for the depressing synapse model, but to obtain a fair comparison of the two models, we varied the value of w for the static synapse model so that the two models exhibited the same postsynaptic firing rates, ν_{out}, given the same presynaptic firing rates, ν_{in}. More specifically, the value of w was adjusted manually for each value of νin sampled until the disagreement between the postsynaptic firing rates of the two models agreed to within a 5% error. The value of w was not changed by >5% from its original value of w = 0.278 during this process.

RESULTS

We begin by considering how the correlation between pair of presynaptic spike trains is transformed by short-term synaptic depression to the correlation between the two synaptic conductances that these spike trains elicit. We next extend these results to the transfer of correlation over a population of

presynaptic inputs to the correlation between a pair of postsynaptic conductances. Finally, we examine how these correlations between synaptic conductances are transferred to postsynaptic spiking correlations.

Throughout this study, we compare a synapse model that exhibits short-term depression to a static nondepressing synapse model. For the depressing synapse model (Vere-Jones 1966; Wang 1999; de la Rocha and Parga 2005; Rosenbaum et al. 2012), each presynaptic neuron makes $M = 5$ functional contacts onto its postsynaptic target. At each presynaptic spike, each readily releasable vesicle is released independently with probability $p_r = 0.3$. Recovery of released vesicles occurs as a Poisson process with rate $1/\tau_u$ where $\tau_u = 700$ ms. For the static synapse model, every presynaptic spike releases the same amount of neurotransmitter. Parameters are chosen so that postsynaptic firing rates for both models is ~15 Hz when the presynaptic rate is 15 Hz (see METHODS for more details on models and parameters).

Correlations between synaptic conductances are weakened and reshaped by synaptic depression. We first consider the correlation between two conductances generated by a single pair of correlated presynaptic spike trains, $x(t)$ and $y(t)$, each with rate $\nu = 15$ Hz (see METHODS and Fig. 1). We assume that these spike trains are Poisson processes and correlated with an exponentially decaying cross-covariance function $C_{\text{in}}(\tau) = 0.05\nu e^{-|\tau|/\tau_{\text{corr}}}$ (Fig. 3, *A* and *B*). The spike count correlation between the presynaptic spike trains increases with the length of the window from $\rho_{\text{in}}(0) = 0$ towards $\lim_{t\to\infty}\rho_{\text{in}}(t) = 0.05$ (Fig. 3*C*).

Closed form expressions for the autocovariance, $A_g(\tau)$, of the synaptic conductance produced by each of these spike trains as well as the cross-covariance function, $C_{gg}(\tau)$, between the two synaptic conductances are given in the METHODS for a depressing and a static synapse model. The Pearson correlation, $\rho_{gg}(t)$, between two conductances over a window of length t is given in terms of integrals of the auto- and cross-covariance functions, cf *Eq. 2*.

For a static, nondepressing synapse model, the auto- and cross-covariance functions of the conductances, $A_g(\tau)$ and $C_{gg}(\tau)$, are positive with central peaks at $\tau = 0$ (Fig. 3, *D* and *E*). The timescale at which the tails of these peaks decay is given by $\max\{\tau_{\text{corr}}, \tau_\alpha\}$ where τ_α is the decay time constant of the synaptic conductance kernels and τ_{corr} is the time constant of the correlations between the presynaptic spike trains (see METHODS; here, $\tau_\alpha = 5$ ms and $\tau_{\text{corr}} = 20$ ms). The Pearson correlation coefficient between the conductances over a window of length t increases with t towards the input spike count correlation, $\lim_{t\to\infty}\rho_{gg}(t) = \lim_{t\to\infty}\rho_{\text{in}}(t) = 0.05$, since a static synapse imposes a linear filter (see Fig. 3, *C* and *F*, METHODS, and Tetzlaff et al. 2008).

The auto- and cross-covariance functions of the conductances produced by a depressing synapse model also have central peaks at $\tau = 0$ with the same initial decay rate as for the static synapse model, but negative temporal correlations are introduced by synaptic depression. These negative correlations decay at the timescale of the exponential part of the kernel, $K(\tau)$ (see METHODS). This timescale, given by $\tau_0 = \tau_u/(1 + p_r\nu\tau_u)$, is typically longer than the timescale of the central peak so that the auto- and cross-covariance functions have a positive central peak at small τ, surrounded by a negative component at larger τ (Fig. 3, *G* and *H*, but the negative temporal correlations are difficult to see in Fig. 3*G* due to the relative amplitude of the exponential peak).

The Pearson correlation, $\rho_{gg}(t)$, between the two conductances produced by the depressing synapse model initially increases with the integration window, t, because of the central peak in $C_{gg}(\tau)$ (Fig. 3*I*). For larger t, negative temporal correlations cause the correlation to decrease. Correlations are drastically smaller for the depressing synapse model than for the nondepressing model. Indeed, synaptic depression reduces the value of $\rho_{gg}(t)$ by a factor of more than 4 for small t and by a factor of >20 for large t (Fig. 3, *F* and *I*, solid curves).

In the limit of large t, the Pearson correlation between the conductances produced by the depressing synapse model is small. This result can be understood intuitively by noting that for $t >> \tau_\alpha$, the correlation, $\rho_{gg}(t)$, between the conductances is equal to the correlation coefficient between the number of vesicles released at each synapse in a window of length t. When $U\nu >> M/\tau_u$, the synapses are depleted in the steady state and the number of vesicles released over a long time window is determined primarily by the number of vesicle recovery events that occur during that time window (de la Rocha and Parga 2005; Rosenbaum et al. 2012). Since recovery events are uncorrelated between the two synapses, the number of vesicles released at different synapses is largely uncorrelated and, therefore, $\rho_{gg}(t)$ is small for large t. This argument suggests that correlations should be smaller when the synapses are more depleted. This observation is confirmed by noting that correlations are smaller for the depressing synapse model when presynaptic rates are higher or when vesicle recovery times are longer (Figs. 3*I* and 4, *A* and *B*).

When τ_u or ν_{in} is small, vesicles are recovered before each presynaptic spike arrives. As a result, the stochastic nature of vesicle recovery does not introduce variability to the synaptic response in this regime. However, the number of vesicles released by each presynaptic spike is random and the variability introduced by this randomness reduces correlations (see Fig. 4, *A* and *B* and Rosenbaum and Josíc 2011).

The correlation between conductances increases with the number of contacts made by a presynaptic neuron (Fig. 4*C*) because a large number of synaptic contacts allows synaptic

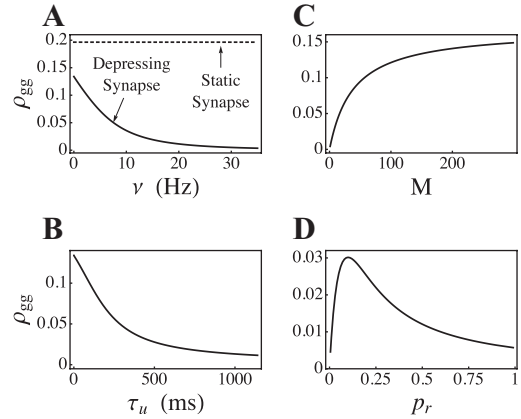

Fig. 4. Dependence of conductance correlation on synaptic parameters. Pearson correlation, $\rho_{gg}(t)$, between two conductances over a window of size t = 1 s, plotted as a function of the presynaptic firing rate (*A*), the recovery time constant (*B*), the number of synaptic contacts (*C*), and the probability (*D*) of release at each contact. Solid lines are from a depressing synapse model and the dashed line in *A* are from a nondepressing, static synapse model.

variability to average out (de la Rocha and Parga 2005; Rosenbaum et al. 2012). Correlations exhibit a nonmonotonic dependence on the probability of release (Fig. 4*D*). A very small probability of release reduces the proportion of nearly synchronous presynaptic spikes that induce nearly synchronous release events, thereby suppressing the correlation of the synaptic response (Rosenbaum and Josíc 2011). A high probability of release depletes the synapses more thoroughly, thereby also decreasing correlations.

Overall, synaptic depression decreases correlations, largely due to the introduction of synaptic variability that is independent across postsynaptic targets. Furthermore, since depression is recruited at higher input firing rates, the amount by which correlations are decreased by synaptic depression depends sensitively on presynaptic firing rates.

Correlations between the conductances produced by two presynaptic populations. We now consider pair of postsynaptic neurons driven by a population of presynaptic spike trains. Two uncoupled postsynaptic neurons each receive synaptic inputs from $n_e = 150$ excitatory and $n_i = 50$ inhibitory Poisson presynaptic spike trains with firing rates $\nu_{in} = 15$. Each pair of presynaptic spike trains is correlated with cross-covariance function $C_{in}(\tau) = 0.05\nu_{in}e^{-|\tau|/\tau_{corr}}$ (see METHODS).

Correlations between individual presynaptic spike trains are weak [$\lim_{t\to\infty}\rho_{in}(t) = 0.05$] but synaptic convergence, i.e., pooling, acts to amplify these correlations so that correlations between the total presynaptic spike counts are much stronger: $\lim_{t\to\infty}\rho_{EE}(t) = 0.89$, $\lim_{t\to\infty}\rho_{II}(t) = 0.72$, and $\lim_{t\to\infty}\rho_{EI}(t) = 0.80$ (see Fig. 5, *A–C*, METHODS, and Renart et al. 2010; Rosenbaum et al. 2011).

For the nondepressing, static synapse model the Pearson correlations between the total excitatory and inhibitory conductances received by each cell increase with the window size, t, over which the correlations are measured (Fig. 5, *D–F*). For large t, the correlation between the conductances approaches the correlation between the presynaptic spike counts, $\lim_{t\to\infty}\rho_{g_Xg_Y}(t) = \lim_{t\to\infty}\rho_{XY}(t)$ for $X, Y \in \{E, I\}$, since the static synapse model imposes a linear filter (see METHODS and Tetzlaff et al. 2008).

For a depressing synapse model, the correlations between the total excitatory and inhibitory conductances initially increase with the window size, t, but begin to decrease for larger t. The timescales of these changes in correlation with window size are the same as those discussed above for an individual pair of conductances. The correlations between the population conductances generated by the depressing synapse model are considerably smaller than the correlations for the static synapse model, especially over large window sizes (Fig. 5, *G–I*).

Thus presynaptic populations can pool their activity and amplify the transfer of correlation to a postsynaptic pair. Nevertheless, the main effects of depression-induced correlation dilution and shaping that was uncovered with a pair of presynaptic cells (Fig. 3) carry over to a model of presynaptic populations.

Postsynaptic spiking correlations are weakened and reshaped by synaptic depression. We now consider two uncoupled postsynaptic neurons driven by the excitatory and inhibitory synaptic conductances considered above. We model these two neurons using a conductance based integrate-and-fire formalism (see METHODS). Since the two postsynaptic cells are uncoupled, correlations between their spiking responses are induced solely through correlations between the synaptic conductances discussed above. We begin by considering a set of parameters for which the pre- and postsynaptic firing rate is approximately $\nu_{in} = 15$ Hz (see METHODS).

The auto- and cross-covariance functions between the postsynaptic spike trains inherit the overall qualitative shape of the auto- and cross-covariance functions between the conductances, except that the postsynaptic autocovariance is negative at small τ due to the absolute and relative refractory periods imposed by the spiking dynamics (Fig. 6, *A*, *B*, *D*, and *E*).

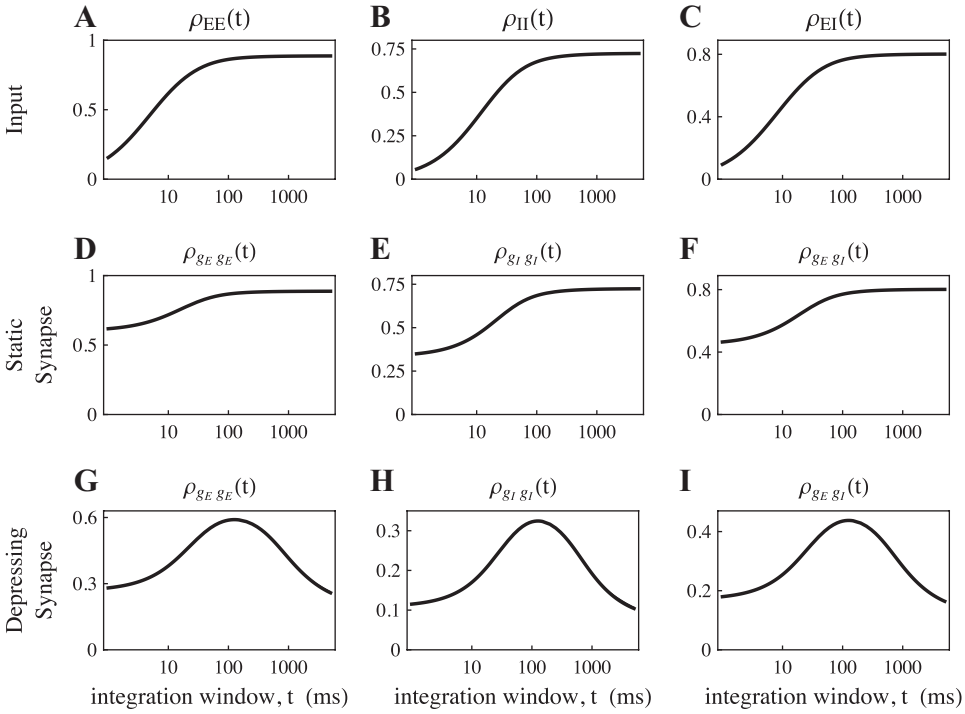

Fig. 5. Short-term depression reduces correlations between population conductances. Correlation coefficient between the two excitatory population spike counts (*A*), between two inhibitory population spike counts (*B*), and between the excitatory and inhibitory population spike counts as a function of window size (*C*). *D–F*: Pearson correlation between the population excitatory and inhibitory conductances produced by the spike trains from *A–C* using a static, nondepressing synapse model. *G–I*: Pearson correlation between the synaptic conductances by the spike trains in *A–C* using a depressing synapse model. Presynaptic excitatory correlations are larger than presynaptic inhibitory correlations at the population level because the excitatory population is larger (see METHODS). Results from Monte Carlo simulations are plotted along with those obtained from the analytical expressions in METHODS, but the two are virtually indistinguishable.

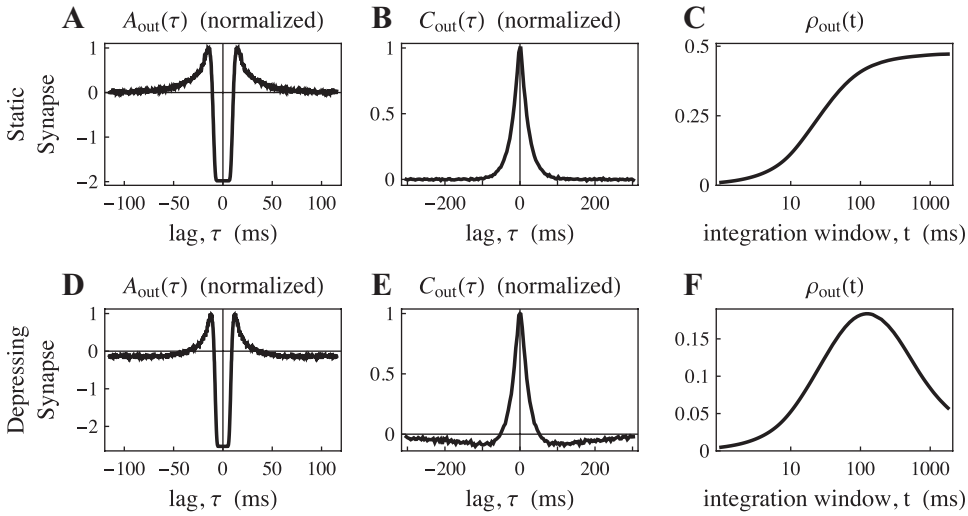

Fig. 6. Short-term depression reduces postsynaptic spiking correlations. Autocovariance (*A*), cross-covariance (*B*), and spike count correlation (*C*) for two postsynaptic spike trains produced by a population of correlated presynaptic neurons using a nondepressing, static synapse model. *D*, *E*, and *F*: same, but for a depressing synapse model. All plots are from Monte Carlo simulations. Firing rates of the neurons is approximately the same for both models (see METHODS), but short-term depression drastically reduces postsynaptic spiking correlations.

Synaptic depression substantially reduces postsynaptic spiking correlations compared with a static synapse, especially over longer time windows (compare Figs. 6, *C* and *F*). This result suggests that short-term depression and stochastic vesicle dynamics provide a mechanism through which small correlations may be maintained in densely connected networks, which complements previously studied mechanisms (Renart et al. 2010; Ecker et al. 2010).

We have shown that correlations between synaptic conductances generated by depressing synapses decrease as the presynaptic firing rate increases (see Fig. 4*A*). Additionally, the correlation susceptibility, defined as the ratio of correlations between synaptic currents to correlations between spiking correlations, is known to increase with postsynaptic firing rates for integrate-and-fire neurons (de la Rocha et al. 2007; Rosenbaum and Josíc 2011). Finally, as presynaptic firing rate increases so does the postsynaptic rate. The combination of these effects yields nonmonotonic changes in postsynaptic spiking correlations as postsynaptic rates are modulated by modulating presynaptic rates: correlations initially increase with firing rate but then decrease at larger rates (Fig. 7, solid line). For a static synapse model, however, spiking correlations mostly increase with firing rate (Fig. 7, dashed line).

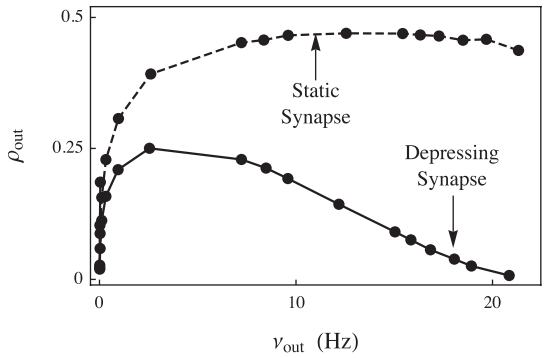

Fig. 7. Short-term depression can cause a nonmonotonic dependence of correlation on firing rate. Postsynaptic spike count correlation, $\rho_{out}(t)$, calculated over a window size of $t = 1$ s plotted as a function of the postsynaptic firing rates, ν_{out}, as the presynaptic rates are varied from $\nu_{in} = 0.05$ Hz to $\nu_{in} = 50$ Hz. Synaptic weights for the static synapse model were adjusted at each sampled point so that the postsynaptic firing rate of the two models agrees to within a 5% error (see METHODS). Error bars are omitted because all standard errors are smaller than radius of the dots.

DISCUSSION

The degree to which spike trains are correlated in the cortex and the mechanisms that determine these correlations are topics of great interest in neural coding (Ecker et al. 2010; Renart et al. 2010; Cohen and Kohn 2011; de la Rocha et al. 2007; Moreno-Bote and Parga 2009; Renart et al. 2010; Rosenbaum et al. 2010; Tchumatchenko et al. 2010; Litwin-Kumar et al. 2011; Rosenbaum and Josíc 2011; Macke et al. 2011; Ly et al. 2012; Trousdale et al. 2012; Ranganathan and Koester 2011; Shlens et al. 2006; Cohen and Maunsell 2009). We used computational modeling and mathematical analysis to show that short-term synaptic depression can drastically reduce correlations between the activity of neurons. In addition, short-term depression shapes the timescale over which these correlations occur (see Figs. 3, 5, and 6). In particular, short-term depression causes correlations over short time windows to be larger than correlations over long time windows, consistent with the findings of at least one experimental study (Giridhar et al. 2011).

Short-term synaptic depression causes a greater reduction in correlations when presynaptic rates are larger (Fig. 4*A*) since higher rates more fully deplete neurotransmitter vesicles. Combined with the fact that correlations are reduced by thresholding mechanisms at low postsynaptic rates (de la Rocha et al. 2007; Rosenbaum and Josíc 2011), this can introduce a nonmonotonic dependence of postsynaptic correlations on postsynaptic rates when presynaptic rates are modulated (Fig. 7). The decrease in spiking correlations at higher firing rates could potentially explain why some experimental studies report a decrease in correlations as rates increase (Cohen and Maunsell 2009, 2011).

The degree to which neuronal activity is correlated in vivo is a topic of active research and debate (Ecker et al. 2010; Renart et al. 2010; Cohen and Kohn 2011). An understanding of the neural mechanisms that modulate correlations is essential to the ongoing discussion of neuronal correlations and their role in the cortical computation. We contribute to this discussion by showing that short-term synaptic depression, which is pervasive in the cortex (Zucker and Regehr 2002), has a substantial impact on the degree to which neural activity is correlated as well as the temporal structure of these correlations.

One previous study (Rosenbaum and Josíc 2011) examined the impact of probabilistic vesicle release on postsynaptic spiking correlations, but the release probabilities used in that study were assumed to be constant and independent of presynaptic spiking history. When presynaptic spike trains are Poisson, a constant probability of release simply scales correlations by the release probability and does not change the timescale over which correlations occur. Thus a model with a constant probability of release does not accurately capture the correlation structure induced by short-term synaptic depression (Fig. 8, dotted line).

A commonly used model of short-term synaptic depression treats the release and recovery of neurotransmitter vesicles as deterministic instead of probabilistic (Tsodyks and Markram 1997; Varela et al. 1997; Chance et al. 1998; Cook et al. 2003; Grande and Spain 2005; Lindner et al. 2009; Merkel and Lindner 2010; Oswald and Urban 2012) and therefore underestimates the variability in the synaptic response. This deterministic model of depression leads to dramatically higher correlation transfer than the case with stochastic depression, as well as a differences in the timescale of transfer (Fig. 8, dashed line). Thus stochastic vesicle dynamics must be accounted for in studies for which neuronal correlations are important.

Our model assumes that each synaptic contact hosts exactly one vesicle docking site, in contrast to similar models in which a single contact can dock multiple vesicles (Vere-Jones 1966; Wang 1999; de la Rocha and Parga 2005; Loebel et al. 2009). This difference could potentially be resolved by interpreting our parameter M as the total number of release sites at all contacts, but this resolution is only consistent if vesicle release at each site is statistically independent. Our mathematical analysis relies on the assumption of independent release at separate functional contacts, so a generalized model would require new analysis or abandoning analytical methods altogether in favor of direct simulation. Simulations show that increasing the number of docking sites per contact while scaling the recovery time constant τ_u accordingly increases synaptic variability and the variability of postsynaptic spiking (de la Rocha and Parga 2005), which could reduce correlations further.

Previous studies have used the stochastic model of short-term synaptic depression used here to explore the impact of synaptic depression on the firing rate of postsynaptic neurons and on the amount of information transmitted through a synapse (Fuhrmann et al. 2002; Goldman 2004). A few studies have also looked at how short-term depression interacts with correlations between presynaptic inputs to determine the response statistics of a single postsynaptic neuron (Goldman et al. 1999, 2002; de la Rocha et al. 2004; de la Rocha and Parga 2005; Rosenbaum et al. 2012), but to the authors' knowledge the question of how short-term synaptic depression and stochastic vesicle dynamics determine correlations between postsynaptic neurons has not been previously investigated.

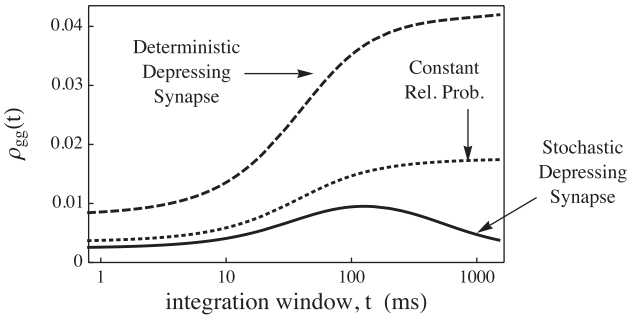

Fig. 8. Deterministic and static probabilistic synapse models transfer correlations differently than a stochastic, depressing synapse model. Pearson correlation between a pair of conductances produced by the spike trains in Fig. 3, *A–C*, using the depressing synapse model described in METHODS (solid line, same as Fig. 3*I*), using a model with a constant vesicle release probability (dotted line), and using a depressing synapse model with deterministic dynamics (dashed line). Parameters were chosen so that all models produce the same mean conductance.

Our results show that short-term synaptic depression and stochastic vesicle dynamics provide a powerful mechanism for the decorrelation of neural activity in feedforward settings. Previous studies show that intrinsic neuronal dynamics (de la Rocha et al. 2007; Rosenbaum and Josíc 2011; Litwin-Kumar et al. 2011; Barreiro et al. 2010; Hong et al. 2012), reciprocal feedback inhibition (Ly et al. 2012; Middleton et al. 2012; Litwin-Kumar et al. 2012; Tetzlaff et al. 2012) and recurrent network dynamics (Hertz 2010; Renart et al. 2010; Pernice et al. 2011; Pernice et al. 2012; Trousdale et al. 2012) also act as decorrelating mechanisms. It is not immediately clear, however, how short-term synaptic depression and stochastic vesicle dynamics interact with recurrent network dynamics to determine correlations. For example, short-term depression could weaken negative feedback loops that promote decorrelation (Tetzlaff et al. 2012; Litwin-Kumar et al. 2012), thereby possibly strengthening correlations. An investigation of the impact of short-term synaptic depression and stochastic vesicle dynamics on correlations in recurrent networks is an important goal for understanding the genesis and role of neuronal correlation in cortex. Our results contribute some fundamental insights that can inform such an investigation, but a complete investigation is outside the scope of this study.

APPENDIX

Here we give equations for the constants that appear in the expressions for the auto- and cross-covariance functions of the conductance produced by the depressing synapse model (see METHODS). All expressions are from (Rosenbaum et al. 2012). The constant D_0 quantifies variability added to the synaptic response by synaptic depression and is given by

$$D_0 = \frac{\nu\tau_u P_r^2}{\nu\tau_u(2 - p_r)p_r + 2}.$$

The kernel, $K(\tau)$, quantifies the filtering properties of synaptic depression and includes a delta function centered at $\tau = 0$ added to a negative exponential. The mass of the delta function, the amplitude of the peak, and the time constant of the exponential are given by

$$A_K = \frac{p_r M}{1 + p_r\nu\tau_u},$$

$$B_K = \frac{p_r^2 M\nu}{1 + p_r\nu\tau_u},$$

and

$$\tau_0 = \frac{\tau_u}{1 + p_r\nu\tau_u}$$

respectively.

The function $F(\tau)$ represents variability introduced by probabilistic vesicle release and stochastic vesicle recovery. The function includes a delta function centered at $\tau = 0$ surrounded by an exponential peak. The time constant of the exponential is τ_0, defined above. The mass of the delta function and the amplitude of the exponential are given by

$$A_F = \frac{D_0 M(2 - 2U + v\tau_0 U^2)}{\tau_0 U(1 + v\tau_u U)}$$

and

$$B_F = \frac{D_0 M v\left[(1 - U)(\tau_u + \tau_0(1 - v\tau_u U)\right]}{\tau_0 \tau_u (1 + v\tau_u U)}$$

respectively.

Finally, the constant c_0 quantifies a scaling of correlations caused by the dynamics of short-term depression and is given by

$$c_0 = \frac{v\tau_u(2 - p_r)p_r + 2}{v\tau_u(2 - cp_r)p_r + 2}c$$

where $c = \lim_{t\to\infty}\rho_{\text{in}}(t)$ is the total input correlation.

ACKNOWLEDGMENTS

We thank the reviewers for many helpful comments.

GRANTS

This work was supported by National Institute of Neurological Disorders and Stroke Grant 1R01-NS-070865-01A1 and National Science Foundation Grants NSF-DMS-1021701 and NSF-DMS-1121784.

DISCLOSURES

No conflicts of interest, financial or otherwise, are declared by the author(s).

REFERENCES

Averbeck B, Latham P, Pouget A. Neural correlations, population coding, computation. *Nat Rev Neurosci* 7: 358–366, 2006.

Bair W, Zohary E, Newsome W. Correlated firing in macaque visual area mt: time scales and relationship to behavior. *J Neurosci* 21: 1676–1697, 2001.

Barreiro A, Shea-Brown E, Thilo E. Time scales of spike-train correlation for neural oscillators with common drive. *Phys Rev E Stat Nonlin Soft Matter Phys* 81: 011916, 2010.

Bäuerle N, Grübel R. Multivariate counting processes: copulas and beyond. *ASTIN Bulletin* 35: 379–408, 2005.

Binder M, Powers R. Relationship between simulated common synaptic input and discharge synchrony in cat spinal motoneurons. *J Neurophysiol* 86: 2266–2275, 2001.

Branco T, Staras K. The probability of neurotransmitter release: variability and feedback control at single synapses. *Nat Rev Neurosci* 10: 373–383, 2009.

Cain N, Shea-Brown E. Computational models of decision making: integration, stability, and noise. *Curr Opinion Neurobiol* 2012 May 14 [Epub ahead of print].

Chance F, Nelson S, Abbott L. Synaptic depression and the temporal response characteristics of v1 cells. *J Neurosci* 18: 4785, 1998.

Cohen M, Kohn A. Measuring and interpreting neuronal correlations. *Nat Neurosci* 14: 811–819, 2011.

Cohen M, Maunsell J. Attention improves performance primarily by reducing interneuronal correlations. *Nat Neurosci* 12: 1594–1600, 2009.

Cohen M, Maunsell J. Using neuronal populations to study the mechanisms underlying spatial and feature attention. *Neuron* 70: 1192–1204, 2011.

Cook DL, Schwindt PC, Grande LA, Spain WJ. Synaptic depression in the localization of sound. *Nature* 421: 66–70, 2003.

Dayan P, Abbott L. *Theoretical Neuroscience: Computational and Mathematical Modeling of Neural Systems*. Cambridge, MA: MIT Press, 2001.

de la Rocha J, Doiron B, Shea-Brown E, Josíc K, Reyes A. Correlation between neural spike trains increases with firing rate. *Nature* 448: 802–806, 2007.

de la Rocha J, Moreno R, Parga N. Correlations modulate the non-monotonic response of a neuron with short-term plasticity. *Neurocomputing* 58: 313–319, 2004.

de la Rocha J, Parga N. Short-term synaptic depression causes a non-monotonic response to correlated stimuli. *J Neurosci* 25: 8416–8431, 2005.

Ecker A, Berens P, Keliris G, Bethge M, Logothetis N, Tolias A. Decorrelated neuronal firing in cortical microcircuits. *Science* 327: 584, 2010.

Fuhrmann G, Segev I, Markram H, Tsodyks M. Coding of temporal information by activity-dependent synapses. *J Neurophysiol* 87: 140, 2002.

Giridhar S, Doiron B, Urban N. Timescale-dependent shaping of correlation by olfactory bulb lateral inhibition. *Proc Natl Acad Sci USA* 108: 5843, 2011.

Goldman M. Enhancement of information transmission efficiency by synaptic failures. *Neural Comput* 16: 1137–1162, 2004.

Goldman M, Maldonado P, Abbott L. Redundancy reduction, and sustained firing with stochastic depressing synapses. *J Neurosci* 22: 584–591, 2002.

Goldman M, Nelson S, Abbott L. Decorrelation of spike trains by synaptic depression. *Neurocomputing* 26: 147–153, 1999.

Grande LA, Spain WJ. Synaptic depression as a timing device. *J Physiol* 20: 201–210, 2005.

Hanson JE, Jaeger D. Short-term plasticity shapes the response to simulated normal and parkinsonian input patterns in the globus pallidus. *J Neurosci* 22: 5164–5172, 2002.

Hertz J. Cross-correlations in high-conductance states of a model cortical network. *Neural Comput* 22: 427–447, 2010.

Hong S, Ratté S, Prescott S, De Schutter E. Single neuron firing properties impact correlation-based population coding. *J Neurosci* 32: 1413–1428, 2012.

Kohn A, Smith M. Stimulus dependence of neuronal correlation in primary visual cortex of the macaque. *J Neurosci* 25: 3661–3673, 2005.

Kuhn A, Aertsen A, Rotter S. Higher-order statistics of input ensembles and the response of simple model neurons. *Neural Comput* 15: 67–101, 2003.

Lampl I, Reichova I, Ferster D. Synchronous membrane potential fluctuations in neurons of the cat visual cortex. *Neuron* 22: 361–374, 1999.

Lindner B, Gangloff D, Longtin A, Lewis JE. Broadband coding with dynamic synapses. *J Neurosci* 29: 2076–2087, 2009.

Litwin-Kumar A, Chacron M, Doiron B. The spatial structure of stimuli shapes the timescale of correlations in population spiking activity. *PLoS Comput Biol* 8: e1002667, 2012.

Litwin-Kumar A, Oswald A, Urban N, Doiron B. Balanced synaptic input shapes the correlation between neural spike trains. *PLoS Comput Biol* 7: e1002305. 2011.

Loebel A, Silberberg G, Helbig D, Markram H, Tsodyks M, Richardson M. Multiquantal release underlies the distribution of synaptic efficacies in the neocortex. *Front Comput Neurosci* 3: 27, 2009.

Ly C, Middleton JW, Doiron B. Cellular and circuit mechanisms maintain low spike covariability and enhance population coding in somatosensory cortex. *Front Comput Neurosci* 6: 7, 2012.

Macke J, Opper M, Bethge M. Common input explains higher-order correlations and entropy in a simple model of neural population activity. *Phys Rev Lett* 106: 208102, 2011.

Markram H. A network of tufted layer 5 pyramidal neurons. *Cereb Cortex* 7: 523–533, 1997.

Mastronarde D. Correlated firing of cat retinal ganglion cells. I. Spontaneously active inputs to x- and y-cells. *J Neurophysiol* 49: 303–324, 1983.

Merkel M, Lindner B. Synaptic filtering of rate-coded information. *Phys Rev E Stat Nonlin Soft Matter Phys* 81: 041921, 2010.

Middleton J, Omar C, Doiron B, Simons D. Neural correlation is stimulus modulated by feedforward inhibitory circuitry. *J Neurosci* 32: 506–518, 2012.

Mitchell J, Sundberg K, Reynolds J. Spatial attention decorrelates intrinsic activity fluctuations in macaque area v4. *Neuron* 63: 879–888, 2009.

Moreno R, de La Rocha J, Renart A, Parga N. Response of spiking neurons to correlated inputs. *Phys Rev Lett* 89: 288101, 2002.

Moreno-Bote R, Parga N. Auto-and crosscorrelograms for the spike response of leaky integrate-and-fire neurons with slow synapses. *Phys Rev Lett* 96: 28101, 2006.

Moreno-Bote R, Parga N. Response of integrate-and-fire neurons to noisy inputs filtered by synapses with arbitrary timescales: firing rate and correlations. *Neural Comput* 10: P237, 2009.

Okun M, Lampl I. Instantaneous correlation of excitation, and inhibition during ongoing and sensory-evoked activities. *Nat Neurosci* 11: 535–537, 2008.

Oswald A, Urban N. Interactions between behaviorally relevant rhythms and synaptic plasticity alter coding in the piriform cortex. *J Neurosci* 32: 6092–6104, 2012.

Pernice V, Staude B, Cardanobile S, Rotter S. How structure determines correlations in neuronal networks. *PLoS Comput Bio* 7: e1002059, 2011.

Pernice V, Staude B, Cardanobile S, Rotter S. Recurrent interactions in spiking networks with arbitrary topology. *Phys Rev E Stat Nonlin Soft Matter Phys* 85: 031916, 2012.

Polk A, Litwin-Kumar A, Doiron B. Correlated neural variability in persistent state networks. *Proc Natl Acad Sci USA* 109: 6295–6300, 2012.

Poulet J, Petersen C. Internal brain state regulates membrane potential synchrony in barrel cortex of behaving mice. *Nature* 454: 881–885, 2008.

Ranganathan G, Koester H. Correlations decrease with propagation of spiking activity in the mouse barrel cortex. *Front Neural Circuits* 5: 8, 2011.

Renart A, de la Rocha J, Bartho P, Hollender L, Parga N, Reyes A, Harris K. The asynchronous state in cortical circuits. *Science* 327: 587–590, 2010.

Romo R, Hernández A, Zainos A, Salinas E. Correlated neuronal discharges that increase coding efficiency during perceptual discrimination. *Neuron* 38: 649–657, 2003.

Rosenbaum R, Josíc K. Mechanisms that modulate the transfer of spiking correlations. *Neural Comput* 23: 1261–1305, 2011.

Rosenbaum R, Rubin J, Doiron B. Short term synaptic depression imposes a frequency dependent filter on synaptic information transfer. *PLoS Comput Biol* 8: e1002557, 2012.

Rosenbaum R, Trousdale J, Josíc K. Pooling and correlated neural activity. *Front Comput Neurosci* 4: 9, 2010.

Rosenbaum R, Trousdale J, Josíc K. The effects of pooling on correlated neural variability. *Front Neurosci* 5: 58, 2011.

Shlens J, Field G, Gauthier J, Grivich M, Petrusca D, Sher A, Litke A, Chichilnisky E. The structure of multi-neuron firing patterns in primate retina. *J Neurosci* 26: 8254–8266, 2006.

Tchumatchenko T, Malyshev A, Geisel T, Volgushev M, Wolf F. Correlations and synchrony in threshold neuron models. *Phys Rev Lett* 104: 058102, 2010.

Tetzlaff T, Helias M, Einevoll G, Diesmann M. Decorrelation of neural-network activity by inhibitory feedback. *PLoS Comput Biol* 8: e1002596, 2012.

Tetzlaff T, Rotter S, Stark E, Abeles M, Aertsen A, Diesmann M. Dependence of neuronal correlations on filter characteristics and marginal spike train statistics. *Neural Comput* 20: 2133–2184, 2008.

Trousdale J, Hu Y, Shea-Brown E, Josíc K. Impact of network structure and cellular response on spike time correlations. *PLoS Comput Biol* 8: e1002408, 2012.

Tsodyks M, Markram H. The neural code between neocortical pyramidal neurons depends on neurotransmitter release probability. *Proc Natl Acad Sci USA* 94: 719, 1997.

Varela JA, Sen K, Gibson J, Fost J, Abbott LF, Nelson SB. A quantitative description of short-term plasticity at excitatory synapses in layer 2/3 of rat primary visual cortex. *J Neurosci* 17: 7926–7940, 1997.

Vere-Jones D. Simple stochastic models for the release of quanta of transmitter from a nerve terminal. *Australian New Zealand J Stat* 8: 53–63, 1966.

Wang XJ. Fast burst firing, and short-term synaptic plasticity: a model of neocortical chattering neurons. *J Neurosci* 89: 347–362, 1999.

Zohary E, Shadlen M, Newsome W. Correlated neuronal discharge rate and its implications for psychophysical performance. *Nature* 370: 140–143, 1994.

Zucker R, Regehr W. Short-term synaptic plasticity. *Annu Rev Physiol* 64: 355–405, 2002.